

See discussions, stats, and author profiles for this publication at: <https://www.researchgate.net/publication/7525704>

# New Class of Verdoheme Analogues with Weakly Coordinating Anions: The Structure of ( $\mu$ -Oxo)bis[(octaethyloxoporphinato)iron(III)] Hexafluorophosphate

ARTICLE in INORGANIC CHEMISTRY · OCTOBER 2005

Impact Factor: 4.76 · DOI: 10.1021/ic050211a · Source: PubMed

---

CITATIONS

10

---

READS

37

7 AUTHORS, INCLUDING:



Meissam Noroozifar

University of Sistan and Baluchestan

85 PUBLICATIONS 742 CITATIONS

SEE PROFILE



Jilla Saffari

University of Sistan and Baluchestan

13 PUBLICATIONS 27 CITATIONS

SEE PROFILE

# New Class of Verdoheme Analogues with Weakly Coordinating Anions: The Structure of $(\mu\text{-Oxo})\text{bis}[(\text{octaethyloxoporphinato})\text{iron(III)}]$ Hexafluorophosphate

Mozhgan Khorasani-Motlagh,<sup>\*,†</sup> Nasser Safari,<sup>‡</sup> Meissam Noroozifar,<sup>†</sup> Jilla Saffari,<sup>†</sup> Mahtab Biabani,<sup>†</sup>  
Júlio S. Rebouças,<sup>§</sup> and Brian O. Patrick<sup>§</sup>

Chemistry Department, University of Sistan & Baluchestan, P.O. Box 98165-181, Zahedan, Iran,  
Chemistry Department, University of Shahid Beheshti, Tehran, Iran, and Chemistry Department,  
University of British Columbia, Vancouver, Canada

Received February 8, 2005

Three new verdoheme analogues with weakly coordinating anions,  $[\text{OEOPFe}^{\text{III}}\text{X}]$ , where OEOP is the monoanion of octaethyloxoporphyrin and  $\text{X} = \text{PF}_6$ ,  $\text{ClO}_4$ , and  $\text{BF}_4$ , have been synthesized and characterized by spectroscopic methods.  $^1\text{H}$  NMR spectroscopy reveals that the  $[\text{OEOPFe}^{\text{III}}\text{X}]$  species are paramagnetic, and the iron is five-coordinate ( $S = 2$ ). The oxidation of  $[\text{OEOPFe}^{\text{II}}\text{PF}_6]$  with dioxygen yields  $[(\text{OEOPFe})_2\text{O}](\text{PF}_6)_2$ . The structure of  $(\mu\text{-oxo})\text{bis}[(\text{octaethyloxoporphinato})\text{iron(III)}]$  has been determined by X-ray diffraction analysis. The eight Fe–N bond distances have an average value of 2.077(3) Å. The oxygen atom sits on the inversion center, and the average axial Fe–O bond length is 1.756(3) Å. The average displacement of the iron(III) atom from the mean porphinato core is 0.60 Å. Crystal data: crystal system, monoclinic;  $a = 8.7114(10)$  Å;  $b = 26.102(4)$  Å;  $c = 15.8323(14)$  Å;  $\beta = 104.134(6)^\circ$ ; space group  $P2_1/c$ ;  $V = 3491.1(7)$  Å<sup>3</sup>;  $Z = 2$ ;  $R1 = 0.0546$ ,  $wR2 = 0.1145$  for data with  $I > 2\sigma(I)$ .

## Introduction

Weakly coordinating anions have been the subject of intensive research in the past decade because of their increasing importance both in organic and inorganic chemistry. Catalytic activities are highly dependent on the type of anion used and increase as the anion becomes less coordinating.<sup>1–3</sup> It is widely recognized that, under certain conditions, the classical “noncoordinating” anions,  $\text{ClO}_4^-$ ,<sup>4</sup>  $\text{BF}_4^-$ ,<sup>5</sup>  $\text{PF}_6^-$ ,<sup>6</sup>  $\text{AsF}_6^-$ ,<sup>7</sup>  $\text{SbF}_6^-$ ,<sup>6a,8</sup> and  $\text{SO}_3\text{F}^-$ ,<sup>9</sup> coordinate to metal ions from all regions of the periodic table. There are

two properties for these weakly coordinating anions. The first is low overall charge, and the second is a high degree of charge delocalization. The charge should be delocalized over the entire anion, so that no individual atom or group of atoms bears a high concentration of charge.<sup>1</sup>

The oxidation of heme in pyridine by dioxygen in the presence of a reducing agent (hydrazine or ascorbic acid) has been used as a model for the heme oxygenase reaction. This process, which is termed coupled oxidation, is generally believed to occur through the sequence of intermediates shown in Scheme 1. The heme is initially hydroxylated at a meso carbon. Subsequently, a green complex (a verdoheme) is formed.  $[\text{OEOPFe}^{\text{III}}\text{X}_2]$ , where OEOP is the monoanion of octaethyloxoporphyrin, is isolated and is well character-

\* To whom correspondence should be addressed. Phone: +98-541-244-6565. Fax: +98-541-244-6888. E-mail: mkhorasani@hamoon.usb.ac.ir.

<sup>†</sup> University of Sistan & Baluchestan.

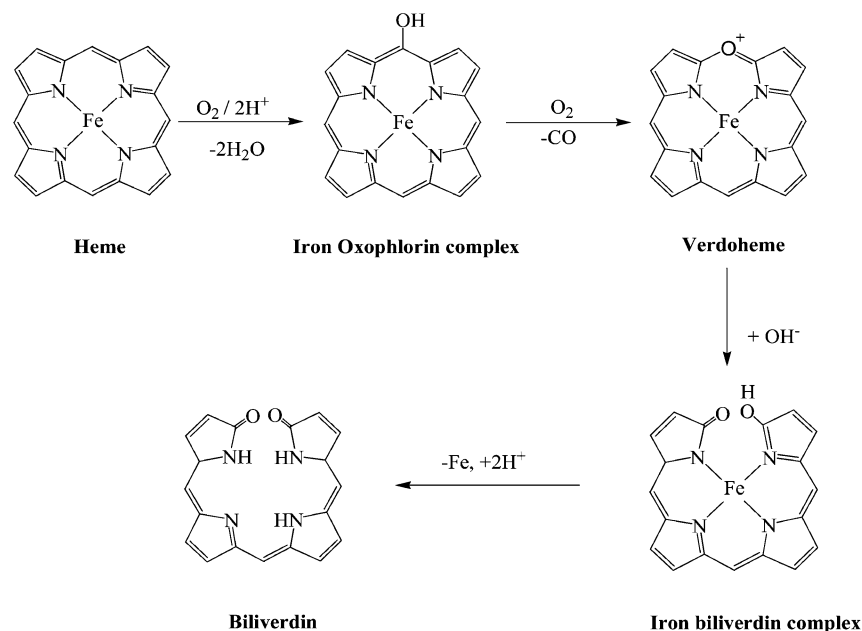
<sup>‡</sup> University of Shahid Beheshti.

<sup>§</sup> University of British Columbia.

- (1) Strauss, S. H. *Chem. Rev.* **1993**, 93, 927–942.
- (2) LaPointe, R. E.; Roof, G. R.; Abboud, K. A.; Klosin, J. J. *Am. Chem. Soc.* **2000**, 122, 9560–9561.
- (3) Beck, W.; Sunkel, K. *Chem. Rev.* **1988**, 88, 1405–1421.
- (4) Reed, C. A.; Mashiko, Y.; Bentley, S. P.; Kastner, M. E.; Scheidt, W. R.; Spartalian, K.; Lang, G. J. *Am. Chem. Soc.* **1979**, 101, 2948–2958.
- (5) (a) Hersh, W. H. *Inorg. Chem.* **1990**, 29, 713–722. (b) Cockman, R. W.; Hoskins, B. F.; McCormick, M. J.; O'Donnell, T. A. *Inorg. Chem.* **1988**, 27, 2742–2745. (c) Hitchcock, P. B.; Lappert, M. F.; Taylor, R. G. J. *Chem. Soc., Chem. Commun.* **1984**, 1082.

- (6) (a) Honeychuck, R. V.; Hersh, W. H. *Inorg. Chem.* **1989**, 28, 2869–2886.
- (7) (a) Klapotke, T.; Thewalt, U. J. *Organomet. Chem.* **1988**, 356, 173–179. (b) Buss, B.; Clegg, W.; Hartmann, G.; Jones, P. G.; Mews, R.; Noltemeyer, M.; Sheldrick, G. M. *J. Chem. Soc., Dalton Trans.* **1981**, 61.
- (8) (a) Hersh, W. H. *J. Am. Chem. Soc.* **1985**, 107, 4599–4601. (b) Shelly, K.; Bartczak, T.; Scheidt, W. R.; Reed, C. A. *Inorg. Chem.* **1985**, 24, 4325–4330.
- (9) Lawrance, G. A. *Chem. Rev.* **1986**, 86, 17–33.

Scheme 1



ized.<sup>10</sup> When X is a halogen, these complexes are high spin, and when X = CN, imidazolate, ..., low spin iron(III) complexes are formed. All of these complexes are autoreduced in the presence of excess amount of pyridine to diamagnetic  $[\text{OEOPFe}^{\text{II}}(\text{py})_2]^+$ .<sup>11–14</sup>

Here, we report the synthesis of three new verdoheme derivatives with weakly coordinating anions,  $[\text{OEOPFe}^{\text{II}}\text{X}]$  (X =  $\text{PF}_6$ ,  $\text{ClO}_4$ ,  $\text{BF}_4$ ). As we will describe later, these anions could stabilize five-coordinate iron(II) with a high-spin ( $S = 2$ ) electronic configuration. Also, we report the synthesis and molecular structure of the novel  $\mu$ -oxo-bridged compound,  $[(\text{OEOPFe}^{\text{III}})_2\text{O}](\text{PF}_6)_2$ . This appears to be the first structural report of dimeric octaethyloxoporphyrin complexes.

## Experimental Section

**General Information.** All reagents and solvents used in this study were purchased from Merck and Aldrich.  $[\text{OEOPFe}^{\text{II}}(\text{py})_2]\text{Cl}$  was synthesized using our previously described method.<sup>10</sup> Solvents were dried by refluxing for several days over Na and benzophenone under Ar and distilled immediately before use. Purified  $\text{N}_2$  (99.999%) was used without further treatment.

NMR experiments were recorded at room temperature (RT,  $\sim 25^\circ\text{C}$ ) on a Bruker AV-500 spectrometer operating at 470.60 MHz

for  $^{19}\text{F}$  (referenced to  $\text{CFCl}_3$ ) using an internal deuterated solvent lock. UV–vis spectra were recorded on a JASCO/7850 spectrometer. IR spectra were recorded as KBr disks on a Shimadzu IR instrument. Elemental analyses were performed by the elemental analysis services of the Chemistry Department of the University of British Columbia.

**Synthesis of  $[\text{OEOPFe}^{\text{II}}\text{PF}_6]$ .** An excess amount of  $\text{NH}_4\text{PF}_6$  (mg) was added to a solution of  $[(\text{OEOP})\text{Fe}^{\text{II}}(\text{py})_2]\text{Cl}$  (20 mg) in dichloromethane (20 mL), and the mixture was stirred for 15 min in air. The solvent was removed under vacuum. The resulting green solid was recrystallized by dissolving it in a minimum volume of dichloromethane, followed by the slow addition of diethyl ether, which precipitated the product as deep green crystals. The solid was dissolved in dichloromethane (25 mL) and HF (5 mL), and methanol (5 mL) was added to the solution, which was then stirred for 5 h under air. The green mixture was filtered to remove any insoluble material, and the filtrate was washed with two 50 mL portions of water. The resulting green solution was dried by passage through a 5 cm thick layer of anhydrous sodium sulfate. The sample was evaporated to dryness under vacuum to give a green residue. The resulting green solid was recrystallized by dissolving it in a minimum volume of dichloromethane and slowly adding diethyl ether to precipitate the product as deep green crystals. Yield: 14 mg, 80%. Anal. Calcd for  $\text{C}_{35}\text{H}_{43}\text{N}_4\text{OFePF}_6$ : C, 57.10; H, 5.84; N, 7.60. Found: C, 56.88; H, 5.44; N, 7.44. UV–vis: 677, 396, 374 nm.  $^1\text{H}$  NMR ( $\text{CDCl}_3$ , relative intensity):  $\delta$  meso-H, 33.18(2), 42.51(1); methylene-H, 34.04(2), 39.47(2), 51.16(2), 53.41(2), 54.69(2), 64.28(2), 65.64(2), 68.44(2); methyl-H, 5.94(6), 7.34(6), 7.93(6), 8.18(6).  $^{19}\text{F}$  NMR ( $\text{CDCl}_3$ , relative intensity):  $\delta$  a doublet at  $-61.44(1)$ ,  $-63.34(1)$ . IR (KBr):  $\nu(\text{PF}_6)$  835, 550  $\text{cm}^{-1}$ .

**Synthesis of  $[\text{OEOPFe}^{\text{II}}\text{ClO}_4]$ .** This was prepared by the procedure used to prepare  $[\text{OEOPFe}^{\text{II}}\text{PF}_6]$ , except that  $\text{HClO}_4$  replaced hydrogen fluoride. Anal. Calcd for  $\text{C}_{35}\text{H}_{43}\text{N}_4\text{OFeClO}_4$ : C, 60.83; H, 6.27; N, 8.11. Found: C, 60.53; H, 5.95; N, 7.95. UV–vis: 673, 358, 304 nm.  $^1\text{H}$  NMR ( $\text{CDCl}_3$ , relative intensity):  $\delta$  meso-H, 38.50(2), 48.41(1); methylene-H, 35.80(2), 43.06(2), 44.30(2), 45.61(2), 56.05(2), 59.07(2), 59.27(2), 65.29(2); methyl-H, 6.30(6), 7.59(6), 7.72(6), 8.20(6). IR (KBr):  $\nu(\text{ClO}_4)$  1140, 1112, 1052, 1010, 973  $\text{cm}^{-1}$ .

- (10) (a) Balch, A. L.; Latos-Grażyński, L.; Noll, B. C.; Olmstead, M. M.; Szterenber, L.; Safari, N. *J. Am. Chem. Soc.* **1993**, *115*, 1422–1429. (b) Medhi, O. K.; Mazumdar, S.; Mitra, S. *Inorg. Chem.* **1989**, *28*, 3243–3248. (c) Collman, J. P.; Brauman, J. I.; Doxsee, K. M.; Halbert, T. R.; Bumenberg, E.; Linder, R. E.; LaMar, G. N.; Gaudio, J. D.; Lang, G.; Spartalian, K. *J. Am. Chem. Soc.* **1980**, *102*, 4182–4192. (d) Koerner, R.; Latos-Grażyński, L.; Balch, A. L. *J. Am. Chem. Soc.* **1998**, *120*, 9246–9255.
- (11) (a) Balch, A. L.; Noll, B. C.; Safari, N. *Inorg. Chem.* **1993**, *32*, 2901–2905. (b) Latos-Grażyński, L.; Noll, B. C.; Olmstead, M. M.; Safari, N. *J. Am. Chem. Soc.* **1993**, *115*, 9056–9061.
- (12) Balch, A. L.; Olmstead, M. M.; Safari, N. *Inorg. Chem.* **1993**, *32*, 291–296.
- (13) Balch, A. L.; Korner, R.; Latos-Grażyński, L.; Lewis, J. E.; St. Claire, T. N.; Zovinka, E. P. *Inorg. Chem.* **1997**, *36*, 3892–3897.
- (14) Balch, A. L.; Noll, B. C.; Olmstead, M. M.; Phillips, S. L. *Inorg. Chem.* **1996**, *35*, 6495–6506.

**Table 1.** Crystallographic Data for [(OEOPFe<sup>II</sup>)<sub>2</sub>O](PF<sub>6</sub>)<sub>2</sub>

formula	C <sub>70</sub> H <sub>86</sub> F <sub>12</sub> Fe <sub>2</sub> N <sub>8</sub> O <sub>3</sub> P <sub>2</sub>
fw	1489.11
cryst syst	monoclinic
space group	<i>P</i> 2 <sub>1</sub> / <i>c</i>
<i>a</i> (Å)	8.7114(10)
<i>b</i> (Å)	26.102(4)
<i>c</i> (Å)	15.8323(14)
$\beta$ (deg)	104.134(6)
<i>V</i> (Å <sup>3</sup> )	3491.1(7)
<i>Z</i>	2
<i>T</i> (K)	173(2)
<i>D</i> (g/cm <sup>3</sup> )	1.417
<i>F</i> (000)	1552
$\lambda$ (Å)	0.71073
$\mu$ (mm <sup>-1</sup> )	0.546
total data collected	39212
final R indices [ <i>I</i> > 2 $\sigma$ ( <i>I</i> )]	R1 = 0.0546, wR2 = 0.1145
final R indices (for all data)	R1 = 0.1058, wR2 = 0.1331
GOF	1.016

**Synthesis of [OEOPFe<sup>III</sup>BF<sub>4</sub>].** This was prepared by the procedure used to prepare [OEOPFe<sup>II</sup>PF<sub>6</sub>], except that NaBF<sub>4</sub> replaced NH<sub>4</sub>PF<sub>6</sub>. Anal. Calcd for C<sub>35</sub>H<sub>43</sub>N<sub>4</sub>OFeBF<sub>4</sub>: C, 61.97; H, 6.39; N, 8.26. Found: C, 61.65; H, 6.10; N, 7.90. UV-vis: 670, 393, 357 nm. <sup>1</sup>H NMR (CDCl<sub>3</sub>, relative intensity):  $\delta$  meso-H, 36.46(2), 50.89(1); methylene-H, 35.45(2), 41.67(2), 48.04(2), 48.50(2), 55.82(2), 61.93(2), 63.47(2), 64.99(2); methyl-H, 6.18(6), 7.51(6), 7.86(6), 8.22(6). IR (KBr):  $\nu$ (BF<sub>4</sub>) 1101, 1063, 1029 cm<sup>-1</sup>.

**Synthesis of [(OEOPFe<sup>III</sup>)<sub>2</sub>O](PF<sub>6</sub>)<sub>2</sub>.** Oxygen was bubbled through a solution of [OEOPFe<sup>II</sup>PF<sub>6</sub>] (20 mg) in dichloromethane (20 mL) for more than 5 h. The sample was evaporated to dryness under vacuum to give a green residue. The resulting green solid was recrystallized by dissolving it in a minimum volume of dichloromethane and slowly adding diethyl ether to precipitate the product as deep green crystals. Anal. Calcd for C<sub>70</sub>H<sub>86</sub>N<sub>8</sub>O<sub>3</sub>-Fe<sub>2</sub>P<sub>2</sub>F<sub>12</sub>: C, 56.46; H, 5.77; N, 7.52. Found: C, 56.18; H, 5.49; N, 7.44. UV-vis: 677, 396, 374 nm. <sup>1</sup>H NMR (CDCl<sub>3</sub>, relative intensity):  $\delta$  methylene-H, 4.58(2), 5.42(2), 5.62(2), 5.74(2), 6.15(2), 6.53(2), 7.01(2), 7.79(2); methyl-H, 1.00–1.16(24). IR (KBr):  $\nu$ (Fe–O–Fe) 863,  $\nu$ (PF<sub>6</sub><sup>-</sup>) 832, 558 cm<sup>-1</sup>. Crystals of [(OEOPFe<sup>III</sup>)<sub>2</sub>O](PF<sub>6</sub>)<sub>2</sub> were suitable for X-ray crystallography.

**X-ray Structure Determination.** Red-brown crystals of [(OEOPFe<sup>II</sup>)<sub>2</sub>O](PF<sub>6</sub>)<sub>2</sub> were grown by diffusion of ether into a dichloromethane solution of [(OEOPFe<sup>II</sup>)<sub>2</sub>O](PF<sub>6</sub>)<sub>2</sub>, and measurements were made on a Bruker  $\times 8$  APEX diffractometer with graphite monochromated Mo K $\alpha$  radiation ( $\lambda$  = 0.71073). The data were collected at a temperature of  $-100 \pm 1$  °C to a maximum  $2\theta$  value of 50.3°. The structure (Figures 3–5) was solved by direct methods<sup>15</sup> and expanded using Fourier techniques.<sup>16</sup> The non-H atoms were refined anisotropically. All hydrogen atoms were included in calculated positions but were not refined. The standard deviation of an observation of unit weight was 1.016. The weighting scheme was based on counting statistics. Plots of  $\sum w(|F_o| - |F_c|)^2$  versus  $|F_o|$ , reflection order in data collection,  $\sin \theta/\lambda$ , and various classes of indices, showed no unusual trends. The maximum and minimum peaks on the final difference Fourier map corresponded to 0.52 and  $-0.45$  e Å<sup>-3</sup>, respectively. Some details of the collection

**Table 2.** Selected Bond Lengths(Å) and Angles (deg) for [(OEOPFe<sup>II</sup>)<sub>2</sub>O](PF<sub>6</sub>)<sub>2</sub>

N1–Fe1	2.048(3)
N2–Fe1	2.073(3)
N3–Fe1	2.061(3)
N4–Fe1	2.051(3)
O1–Fe1	1.7644(5)
O1–Fe1	1.7644(5)
C9–O10	1.347(4)
C11–O10	1.364(4)
Fe1–O1–Fe1	180.00(3)
O1–Fe1–N1	109.48(8)
O1–Fe1–N4	104.63(8)
O1–Fe1–N3	100.48(8)
O1–Fe1–N2	104.58(8)
N1–Fe1–N4	87.58(11)
N4–Fe1–N2	150.45(11)
N3–Fe1–N2	83.89(11)
C1–N1–Fe1	127.1(2)
C4–N1–Fe1	127.5(2)
C9–N2–Fe1	127.4(2)
C6–N2–Fe1	126.4(2)
C11–N3–Fe1	126.9(2)
C14–N3–Fe1	126.0(2)
C19–N4–Fe1	126.1(2)
C16–N4–Fe1	125.9(2)

are given in Table 1. Selected bond lengths and angles are given in Table 2.

## Results

Verdohemochrome, [OEOPFe<sup>II</sup>(py)<sub>2</sub>]Cl, is prepared from [OEOPFe<sup>II</sup>(py)<sub>2</sub>].<sup>10</sup> The treatment of [OEOPFe<sup>II</sup>(py)<sub>2</sub>]Cl with excess NH<sub>4</sub>PF<sub>6</sub> in air yields [(OEOP)Fe<sup>II</sup>(py)<sub>2</sub>]PF<sub>6</sub> which reacts with HX (X = F, ClO<sub>4</sub>) to produce [OEOPFe<sup>II</sup>X] (X = PF<sub>6</sub>, ClO<sub>4</sub>). Also, treatment of [OEOPFe<sup>II</sup>(py)<sub>2</sub>]Cl with excess NaBF<sub>4</sub> in air yields [(OEOP)Fe<sup>II</sup>(py)<sub>2</sub>]BF<sub>4</sub>, which reacts with hydrogen fluoride to produce [OEOPFe<sup>II</sup>BF<sub>4</sub>]. The [OEOPFe<sup>II</sup>X] species (X = PF<sub>6</sub>, ClO<sub>4</sub>, BF<sub>4</sub>) were obtained as stable green crystals in the presence of oxygen and had good solubility in chloroform and dichloromethane.

The UV-vis spectra of dichloromethane solutions of [OEOPFe<sup>II</sup>X] (X = PF<sub>6</sub>, ClO<sub>4</sub>, BF<sub>4</sub>), while clearly different from those of [OEOPFe<sup>III</sup>Cl<sub>2</sub>], are very similar to those of other iron(II) complexes of octaethyloxoporphyrin, such as [OEOPFe<sup>II</sup>Cl].<sup>10</sup> The electronic absorption spectrum of [OEOPFe<sup>II</sup>PF<sub>6</sub>] in dichloromethane is shown in Figure 1a. When pyridine is added to dichloromethane solutions of [OEOPFe<sup>II</sup>X] (X = PF<sub>6</sub>, ClO<sub>4</sub>, BF<sub>4</sub>), a compound analogous to the starting material [OEOPFe<sup>II</sup>(py)<sub>2</sub>]<sup>+</sup> is formed, as revealed by UV-vis analyses. Figure 1b illustrates the in situ formation of [OEOPFe<sup>II</sup>(py)<sub>2</sub>]PF<sub>6</sub> from [OEOPFe<sup>II</sup>PF<sub>6</sub>]. If HCl is added to aerobic dichloromethane solutions of these complexes, [OEOPFe<sup>III</sup>Cl<sub>2</sub>]<sup>10</sup> is formed. These in situ reactions have been monitored by UV-vis spectroscopy and are summarized in Scheme 2.

The [OEOPFe<sup>II</sup>X] species (X = PF<sub>6</sub>, ClO<sub>4</sub>, BF<sub>4</sub>) were also characterized by infrared spectroscopy. The vibrations from the PF<sub>6</sub> group for [OEOPFe<sup>II</sup>PF<sub>6</sub>] appear at 835 and 550 cm<sup>-1</sup> and are in agreement with those at 830 and 550 cm<sup>-1</sup> reported for [TPPFePF<sub>6</sub>].<sup>4</sup> The vibrations from the ClO<sub>4</sub> group for [OEOPFe<sup>II</sup>ClO<sub>4</sub>] appear at 1140, 1112, 1052, 1010, and 973 cm<sup>-1</sup>. The  $\nu$ (ClO<sub>4</sub>) values in this complex are similar to those

(15) Altomare, A.; Burla, M. C.; Cammelli, G.; Cascarano, M.; Gaiacovazzo, C.; Guagliardi, A.; Moliterni, A. G. G.; Polidori, G.; Spanga, A. *J. Appl. Crystallogr.* **1999**, 32, 115.

(16) Beurskens, P. T.; Admirals, G.; Beurskens, G.; Bosman, W. P.; de Gelder, R.; Israel, R.; Smits, J. M. M. *The DIRDIF94 Program System, Technical Report of the Crystallography Laboratory*; University of Nijmegen: Nijmegen, The Netherlands, 1994.

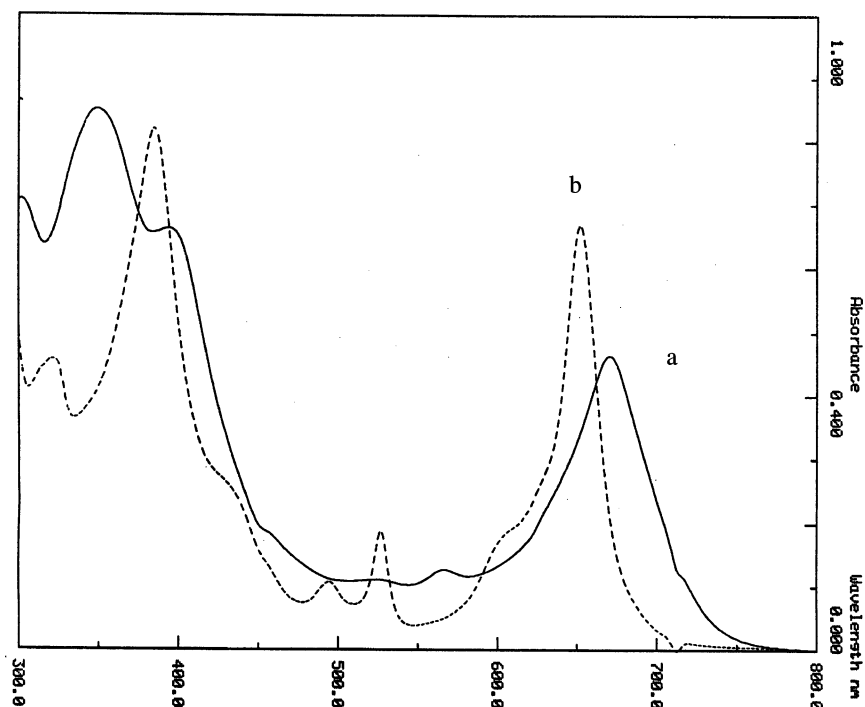
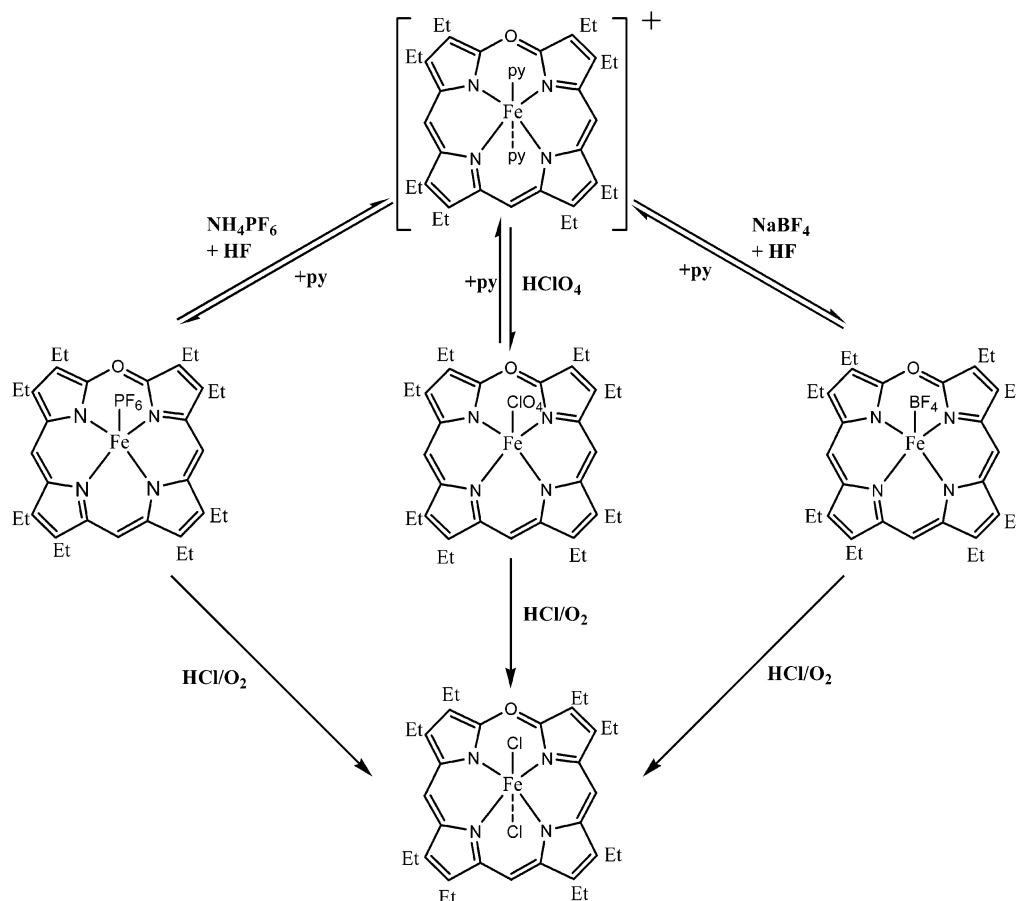


**Figure 1.** UV-vis absorption spectra of (a) [OEOPFe<sup>II</sup>PF<sub>6</sub>] in dichloromethane and (b) [OEOPFe<sup>II</sup>PF<sub>6</sub>] in dichloromethane after the addition of 1% pyridine.

**Scheme 2**



of a related species, namely [TPPFe(OCIO<sub>3</sub>)],<sup>4</sup> which has bands at 1170, 1150, 1120, 840, and 610 cm<sup>-1</sup>. Of note, the structure of [TPPFe(OCIO<sub>3</sub>)] is known and reveals that the perchlorato ligand is monodentate with an unusually short

Fe—O distance.<sup>4</sup> The vibrations resulting from the BF<sub>4</sub> group for [OEOPFe<sup>II</sup>BF<sub>4</sub>] appear at 1101, 1063, and 1029 cm<sup>-1</sup>, and these values are close to those at 1070 and 1050 cm<sup>-1</sup> reported for [TPPFeBF<sub>4</sub>].<sup>4</sup>



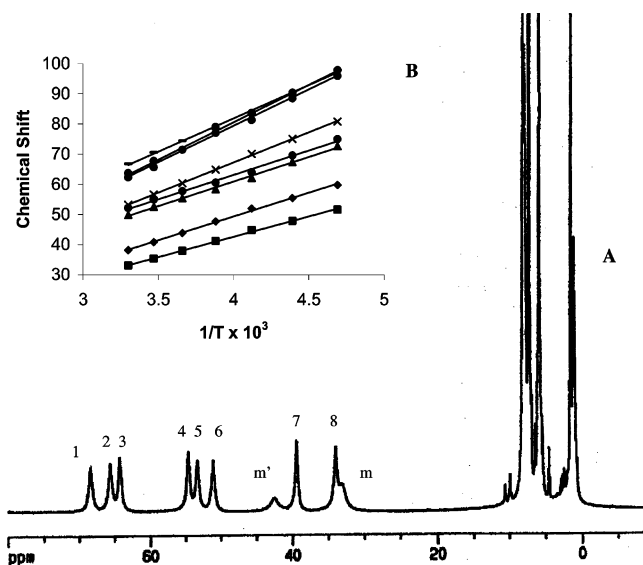


**Figure 2.** (A) 500 MHz  $^1\text{H}$  NMR spectrum of  $[\text{OEOPFe}^{\text{II}}\text{PF}_6]$  in chloroform- $d$  at RT. Resonances are identified as m,  $m'$  = meso protons, and the resonances of the methylene protons are numbered 1–8. (B) A plot of the chemical shifts vs  $T^{-1}$  for the methylene proton resonances.

The  $[\text{OEOPFe}^{\text{II}}\text{X}]$  species ( $\text{X} = \text{PF}_6$ ,  $\text{ClO}_4$ ,  $\text{BF}_4$ ) are paramagnetic. Their magnetic moments in chloroform solution at 25  $^\circ\text{C}$ , as measured by the Evans' technique,<sup>17</sup> are 4.73, 4.84, and 4.85  $\mu_{\text{B}}$ , respectively. This is consistent with a high-spin ( $S = 2$ ) electronic configuration for these complexes.

All resonances in the  $^1\text{H}$  NMR spectrum of the  $[\text{OEOPFe}^{\text{II}}\text{X}]$  species ( $\text{X} = \text{PF}_6$ ,  $\text{ClO}_4$ ,  $\text{BF}_4$ ) are well spread out and were assigned on the basis of their intensities, line widths, and chemical shifts at room temperature. The  $^1\text{H}$  NMR spectra of these species are similar to each other and Figure 2 shows, for example, the spectrum of  $[\text{OEOPFe}^{\text{II}}\text{PF}_6]$  in  $\text{CDCl}_3$  at 25  $^\circ\text{C}$ . The methylene and methine protons show strong paramagnetic shifts that place them in the downfield region. The two methine resonances observed in the spectrum of each of these complexes show an intensity ratio of 1:2 and greater line widths, which is consistent with the fact that they are the protons closest to the iron center and hence that they are the most affected by dipolar relaxation. There are eight clearly resolved, equally intense, methylene resonances that span a wide range from 30 to 70 ppm. Since the iron is five-coordinate (vide infra), each of the two methylene protons of the four unique ethyl groups is chemically distinct, which results in eight signals for the methylene resonances. Four methyl resonances are seen in the 6–8 ppm region. Also worth mentioning is that the line widths increase in the order methyl > methylene > meso. This is consistent with a dominant dipolar contribution to the line width (which is proportional to  $r^{-6}$ )<sup>18</sup> because the distance between the oxoporphyrin protons and the iron center follow an inverse order (i.e., meso > methylene > methyl). These spectra are consistent with the structure shown in Scheme 2, in which the iron is five-coordinate and each of the two methylene protons of the four unique ethyl

groups is chemically distinct, and hence there are eight methylene resonances. The temperature dependence of the  $^1\text{H}$  NMR spectrum shows the linear behavior of the chemical shifts when these are plotted versus  $T^{-1}$ . This is shown for  $[\text{OEOPFe}^{\text{II}}\text{PF}_6]$  in inset B of Figure 2. However, the chemical shifts do not extrapolate at infinite temperature to the positions anticipated for a diamagnetic material.

The  $^{19}\text{F}$  NMR spectrum of  $[(\text{OEOP})\text{FePF}_6]$  shows a broad doublet ( $\Delta\nu_{1/2} = 274$  Hz) at  $-62.67$  ppm with  $J_{\text{P-F}} = 681.41$  Hz. Of note, the corresponding chemical shift and coupling constant for  $\text{AgPF}_6$  are  $-72.84$  ppm and 712.9 Hz, respectively.<sup>19</sup> The  $^{19}\text{F}$  NMR spectrum of  $[\text{OEOPFe}^{\text{II}}\text{BF}_4]$  shows a very broad peak centered at  $-163.5$  ppm, whose value is close to that reported for  $[\text{VO}(\text{salen})\text{BF}_4]$ , which contains a coordinated  $\text{BF}_4$  moiety.<sup>20</sup>

The  $[(\text{OEOP})\text{FePF}_6]$  complex in dichloromethane reacts with oxygen within 5 h to yield the  $[(\text{OEOPFe})_2\text{O}](\text{PF}_6)_2$  species. The progress of the reaction may be monitored by UV–vis spectroscopy, and if oxygen is replaced with air, the reaction takes 2 days to go to completion. It is worth mentioning that the UV–vis spectrum of  $[(\text{OEOPFe})_2\text{O}](\text{PF}_6)_2$  is similar to that reported for iron(III) octaethyloxoporphyrin complexes.

The infrared spectra of binuclear oxygen-bridged species have been well studied and the frequency of the asymmetric  $\text{M-O-M}$  vibration is around 700–900  $\text{cm}^{-1}$ .<sup>21</sup> For example, asymmetric  $\text{Fe-O-Fe}$  stretch bands appears at 885 and 870  $\text{cm}^{-1}$  for  $[\text{TPPFe}]_2\text{O}$ <sup>22</sup> and at 877  $\text{cm}^{-1}$  for  $[\text{OEOPFe}]_2\text{O}$ .<sup>23</sup> A strong broad band with a shoulder is observed in the infrared spectrum of  $[(\text{OEOPFe})_2\text{O}](\text{PF}_6)_2$  in the 820–870  $\text{cm}^{-1}$  region. This may result from an overlap between the band associated with the asymmetric  $\text{Fe-O-Fe}$  stretch (863  $\text{cm}^{-1}$ ) and that of the  $\text{PF}_6$  moiety vibration (832  $\text{cm}^{-1}$ ).

The  $^1\text{H}$  NMR spectrum of  $[(\text{OEOPFe})_2\text{O}](\text{PF}_6)_2$  revealed one broad methyl resonance in the range of 1.00–1.16 ppm and eight, clearly resolved, equally intense methylene resonances at 4.58, 5.42, 5.62, 5.74, 6.15, 6.53, 7.01, and 7.79 ppm (Figure 3). The two meso resonances are not well-resolved and are probably hidden under the methylene resonances. Thus, each iron octaethyloxoporphyrin moiety within the dimer should possess the same microsymmetry as the corresponding five-coordinate monomer. Although broad, all of the  $^1\text{H}$  NMR resonances have chemical shifts that fall within the diamagnetic pocket. The magnetic moment of  $[(\text{OEOPFe})_2\text{O}](\text{PF}_6)_2$ , as well as the  $^1\text{H}$  NMR, indicates that this complex contains two antiferromagnetically coupled high-spin iron(III) centers similar to those of the well-known ( $\mu$ -oxo)iron(III) porphyrin dimers.<sup>24–26</sup>

(17) Evans, D. F. *J. Chem. Soc.* **1959**, 2003–2005.

- (18) Swift, T. J. In *NMR of Paramagnetic Molecules*; Academic Press: New York, 1973; p 23.  
 (19) Fernandez-Galan, R.; Manzano, B. R.; Otero, A.; Lanfranchi, M.; Pellinghelli, M. A. *Inorg. Chem.* **1994**, *33*, 2309–2312.  
 (20) Oyaizu, K.; Dewi, E. L.; Tsuchida, E. *Inorg. Chem.* **2003**, *42*, 1070.  
 (21) Summerville, D. A.; Cohen, I. A. *J. Am. Chem. Soc.* **1976**, *98*, 1747–1752.  
 (22) Cohen, I. A. *J. Am. Chem. Soc.* **1969**, *91*, 1980–1983.  
 (23) Cheng, B.; Hobbs, J. D.; Debrunner, P. G.; Erlebacher, J.; Shelnutt, J. A.; Scheidt, W. R. *Inorg. Chem.* **1995**, *34*, 102–110.  
 (24) La Mar, G. N.; Eaton, G. R.; Holm, R. H.; Walker, F. A. *J. Am. Chem. Soc.* **1973**, *95*, 63–75.

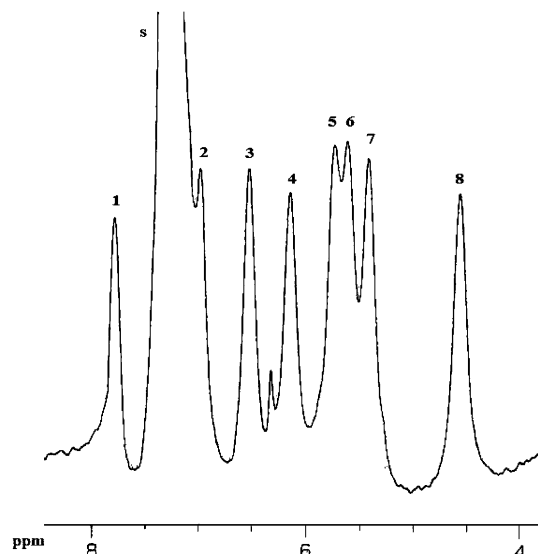


**Figure 3.**  $^1\text{H}$  NMR spectrum (methylene region) of  $[(\text{OEOPFe})_2\text{O}](\text{PF}_6)_2$  in chloroform- $d$  at RT. The resonances of the methylene protons are numbered 1–8; s = solvent.

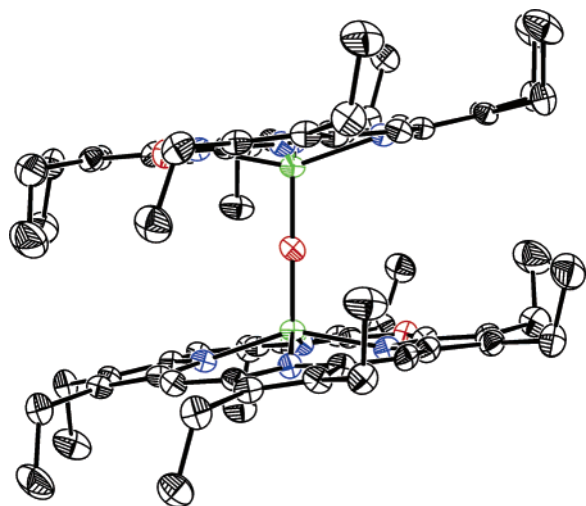


**Figure 4.** ORTEP diagram of the structure of  $[(\text{OEOPFe})_2\text{O}](\text{PF}_6)_2$ . The Fe–O–Fe axis coincides with the plane of paper. Porphyrin hydrogen atoms are omitted for clarity. The atoms were drawn with 50% probability ellipsoids.

Crystals of  $[(\text{OEOPFe}^{\text{III}})_2\text{O}](\text{PF}_6)_2$  suitable for X-ray crystallography were prepared by the slow diffusion of diethyl ether into a dichloromethane solution of the complex.

**Molecular Structure.** The structure of  $(\mu\text{-oxo})\text{bis}[(\text{octaethylxoporphinato})\text{iron}(\text{III})]$ ,  $[(\text{OEOPFe})_2\text{O}](\text{PF}_6)_2$ , has been determined by X-ray crystallography, and some of the crystallographic data are summarized in Table 1. ORTEP diagrams of the monoclinic  $[(\text{OEOPFe})_2\text{O}](\text{PF}_6)_2$  species with eclipsed configuration are shown in Figures 4 and 5. Figure 6 shows the molecular packing of the  $\mu\text{-oxo}$  dimer with  $\text{PF}_6$  groups as counterions. Selected bond distances and angles for  $[(\text{OEOPFe})_2\text{O}](\text{PF}_6)_2$  are given in Table 2. The oxygen atom sits on the inversion center, and the average axial Fe–O bond length is 1.756(3) Å. The Fe–N bond distances have

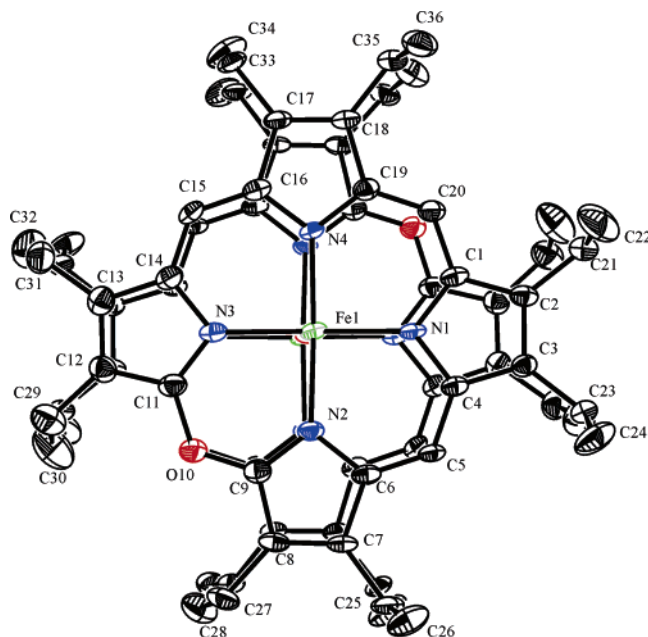


**Figure 5.** "Topview" of monoclinic  $[(\text{OEOPFe})_2\text{O}](\text{PF}_6)_2$  with the Fe(1)–Fe(2) axis perpendicular to the plane of the paper.

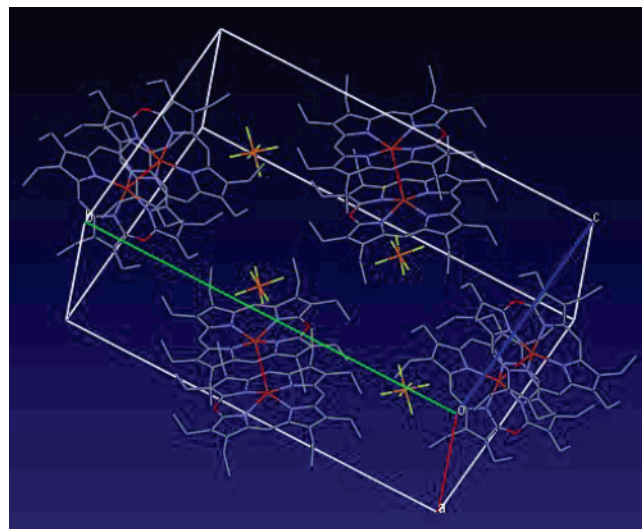


**Figure 6.** Overview of the molecular packing in the crystal structure of  $[(\text{OEOPFe})_2\text{O}](\text{PF}_6)_2$ .

average value of 2.077(3) Å. The average displacement of the iron(III) atom from the mean oxoporphinato core is 0.60 Å. The average mean plane separation is 4.7 Å. These structural parameters are typical for five-coordinate high-spin iron(III) porphyrin dimers.<sup>26</sup>

## Discussion

Despite the fact that the oxoporphyrin is geometrically similar to a porphyrin, it differs in its net charge, since it is a monoanion in its deprotonated form. As a consequence of its lower charge, its neutral complexes have electrostatic requirements different from those of the corresponding porphyrin complexes. Thus, porphyrins form five-coordinate high-spin iron(III) halo complexes ( $\text{PFe}^{\text{III}}\text{Cl}$ ), whereas the oxoporphyrin forms six-coordinate high-spin complexes. In this regard, the oxoporphyrin resembles other porphyrins

(25) Hoffman, A. B.; Collins, D. M.; Day, V. W.; Fleischer, E. B.; Srivastava, T. S.; Hoard, J. L. *J. Am. Chem. Soc.* **1972**, *94*, 3620–3626.

(26) Scheidt, W. R.; Reed, C. A. *Chem. Rev.* **1981**, *81*, 543–555.

**Table 3.** Selected Structural Features for Monobridged Binuclear Iron Porphyrin Complexes

compound	M–Np (Å)	M–Y <sup>a</sup> (Å)	M–Y–M (deg)	$\Delta^b$ (Å)	mean plane separation <sup>c</sup> (Å)	interplanar angle <sup>d</sup> (deg)	twist angle <sup>e</sup> (deg)	ref
[Fe(TPP)] <sub>2</sub> O	2.087(3)	1.763(1)	174.5(1)	0.54	4.50	3.7	35.4	25
[Fe(TPC)] <sub>2</sub> O	2.084(7)	1.755(11)	180.0	0.55	4.60	0.0	30.2	29
[Fe(TPP)] <sub>2</sub> N	1.991(3)	1.661(7)	180.0	0.41	4.1	0.0	31.7	30
[Fe(OEP)] <sub>2</sub> O (triclinic)	2.077(3)	1.756(3)	172.2(2)	0.50	4.5	7.3	17.0	23
[Fe(OEP)] <sub>2</sub> O (monoclinic)	2.080(5)	1.755(10)	176.2(2)	0.54	4.6	2.7	16.8	23
[Fe(OEP)] <sub>2</sub> OH <sup>+</sup>	2.037(10)	1.938(3)	146.2(2)	0.44	<i>f</i>	<i>f</i>	8.6	31
[Fe(OEOP)] <sub>2</sub> O <sup>2+</sup>	2.058(3)	1.764 (5)	180.0	0.60	4.7	0.0	3.2	this work

<sup>a</sup> Y is the bridging ligand. <sup>b</sup> The average displacement of the metal centers from the 24-atom cores. <sup>c</sup> The average mean plane separation for the two porphyrin cores of the dimer. <sup>d</sup> The interplanar angle between the two mean planes of the porphyrin dimer. <sup>e</sup> Average of the four N–Fe–Fe'–N' twist angles. <sup>f</sup> Information not available in the original publication.

which have peripheral substituents that bear a positive charge. Iron(II) porphyrins have a low affinity for axial coordination of halide ions, whereas the neutral five-coordinate oxoporphyrin complexes [OEOPFe<sup>II</sup>X] (X = Cl,<sup>10</sup> PF<sub>6</sub>, ClO<sub>4</sub>, BF<sub>4</sub>) are readily isolated. It is important to note that it is probably overall charge, rather than core charge, which is responsible for the formation of these five-coordinate iron(II) oxoporphyrin complexes.

The UV–vis spectra of the [OEOPFe<sup>II</sup>X] species (X = PF<sub>6</sub>, ClO<sub>4</sub>, BF<sub>4</sub>) are very similar to the analogous [OEOPFe<sup>II</sup>Cl] complex,<sup>10</sup> and the magnetic moment for all of these compounds are consistent with a high-spin (*S* = 2) electronic configuration.

The <sup>1</sup>H NMR spectra of [OEOPFe<sup>II</sup>X] (X = PF<sub>6</sub>, ClO<sub>4</sub>, BF<sub>4</sub>) differ from those of the iron(III) complexes, particularly in their greater complexity, which results from their lower symmetry. This produces eight methylene resonances for the five-coordinate iron(II) complexes, whereas only four are observed for the six-coordinate iron(III) compounds.

The <sup>1</sup>H NMR signals of the [OEOPFe<sup>II</sup>X] species (X = PF<sub>6</sub>, ClO<sub>4</sub>, BF<sub>4</sub>) are significantly downfield shifted with respect to those of the [OEOPFe<sup>II</sup>Cl] species. This is likely a result of the weak coordinating ability of PF<sub>6</sub><sup>–</sup>, ClO<sub>4</sub><sup>–</sup>, and BF<sub>4</sub><sup>–</sup> compared to that of Cl,<sup>27</sup> as it is well established that porphyrin isotropic shifts are very sensitive to the nature of the axial ligands. Indeed, whereas Cl ligands are known to remove the Fe center from the porphyrin plane,<sup>10</sup> it is likely that in [OEOPFe<sup>II</sup>X] species containing weakly coordinating ligands, such as PF<sub>6</sub>, ClO<sub>4</sub>, or BF<sub>4</sub>, the Fe center is supposed to be closer to the porphyrin core, increasing the overlap between the Fe and the oxoporphyrin orbitals. This could provide an efficient route for delocalization of the spin density within the ring and, ultimately, explain the higher downfield isotropic shift of the [OEOPFe<sup>II</sup>X] species (X = PF<sub>6</sub>, ClO<sub>4</sub>, BF<sub>4</sub>) relative to those of OEOPFe<sup>II</sup>Cl. It is also worth noticing that, in a limiting situation, [OEOPFe<sup>II</sup>X] species containing weakly coordinating anions would resemble four-coordinate iron(II) porphyrins more closely than five-coordinate ones. Such a situation would be inverted with the increase in the coordinating ability of X, which may approximate the spectral features of

[OEOPFe<sup>II</sup>Cl] to those of five-coordinate iron(II) porphyrins. Indeed, four-coordinate iron(II) porphyrins show higher isotropic shifts than the ones observed for five-coordinate analogues.<sup>10b</sup>

On the basis of information from the Cambridge Structural Database<sup>28</sup> for the set of complexes that contain an N<sub>4</sub>Fe<sup>III</sup>–O–Fe<sup>III</sup>N<sub>4</sub> unit the Fe–O–Fe angles vary from 143 to 180°, but for simple porphyrins the range is smaller, 166–178°. Selected structural features for some monobridged binuclear iron porphyrin complexes are listed in Table 3. Differences are seen in the bending about the Fe–O–Fe moiety in these complexes. Whereas the Fe–O–Fe moiety is linear in  $\mu$ -O[Fe<sup>III</sup>(OEOP)]<sub>2</sub><sup>2+</sup>, the Fe–O–Fe angle in the closely related complex  $\mu$ -O[Fe<sup>III</sup>(OEP)]<sub>2</sub> is slightly bent to 172.16(17)° (triclinic form) or 176.2(2)° (monoclinic form). The relative (inward/outward) orientations of the peripheral ethyl groups (Figure 4) have been identified as important contributors to the relative orientations of the two porphyrins and the Fe–O–Fe angles in  $\mu$ -oxo dimers. In the case of [(OEOPFe)<sub>2</sub>O]PF<sub>6</sub>, four consecutive ethyl groups on each porphyrin are directed outward relative to the  $\mu$ -oxo moiety, whereas the remaining four ethyl groups are directed inward.

The linear configuration of the Fe–O–Fe moiety in [(OEOPFe)<sub>2</sub>O](PF<sub>6</sub>)<sub>2</sub> is consistent the  $\mu$ -oxo formulation, as a considerably smaller angle for the Fe–O–Fe moiety would be expected in case of  $\mu$ -hydroxo species, such as in  $\mu$ -OH-[Fe<sup>III</sup>(OEP)]<sub>2</sub><sup>+</sup>, for which this angle is only 146.2(2)°.

One measurement that allows for a relatively easy comparison of ring–ring orientation is that of the averaged N–Fe–Fe'–N' twist angle; deviations from 0° occur if the two rings are not exactly parallel. Table 3 also lists the values of the twist angles for a series of singly bridged iron porphyrins. The twist angles observed for most of these  $\mu$ -oxo diiron(III) meso-substituted tetra-arylporphyrin derivatives are 30–35°. The relatively large twist angle is surely the result of minimizing interactions between the bulky peripheral aryl groups. All derivatives with only ethyl groups at the periphery are seen to have twist angles in the range 17–23°, which are significantly smaller than those of the meso-substituted derivatives.<sup>23</sup> The averaged N–Fe–Fe'–N' twist angle for  $\mu$ -O[Fe<sup>III</sup>(OEOP)]<sub>2</sub><sup>2+</sup> is 3.2°, which is much

(27) (a) Evans, D. R.; Reed, C. A. *J. Am. Chem. Soc.* **2000**, *122*, 4660–4667. (b) Reed, C. A.; Guiset, F. *J. Am. Chem. Soc.* **1996**, *118*, 3281–3282.

(28) Lee, H. M.; Olmstead, M. M.; Gross, G. G.; Balch, A. L. *Cryst. Growth Des.* **2003**, *3*, 691–697.



smaller than the other complexes and is consistent with the centrosymmetric nature of the  $\mu\text{-O}[\text{Fe}^{\text{III}}(\text{OEP})]_2^{2+}$  moiety.

The Fe–O bond length in  $[(\text{OEPFe})_2\text{O}]^{2+}$  is 1.7644(5) Å, a value that is comparable to those of the  $\mu\text{-O}[\text{Fe}^{\text{III}}(\text{OEP})]_2$  species, but it is significantly shorter than those of any ( $\mu$ -hydroxo)diiron(III) complexes, whose values range from 1.96 to 2.06 Å.<sup>31</sup>

The average Fe–N distance of 2.058 Å in  $[(\text{OEPFe})_2\text{O}]^{2+}$  is close to the 2.060–2.087 Å range expected for similar high-spin five-coordinate iron porphyrin complexes,<sup>26</sup> but slightly shorter than the values of reported for the analogous OEP-based species,  $\mu\text{-O}[\text{Fe}^{\text{III}}(\text{OEP})]_2$  (2.077 and 2.080 Å for the triclinic and monoclinic forms, respectively). All these values are, however, longer than 2.037 Å, which is reported for the  $\mu\text{-OH}[\text{Fe}^{\text{III}}(\text{OEP})]_2$  species.

Although the structures of some octaethyloxoporphyrin iron complexes, such as  $[\text{OEPFeCl}_2]$  and  $[\text{OEPFeCl}]$ ,<sup>10</sup> display disorder in the location of the oxygen atom and one of the meso methine groups, this is not the case in  $\mu\text{-O}[\text{Fe}^{\text{III}}(\text{OEP})]_2^{2+}$ ; of note, the C<sub>9</sub>–O<sub>10</sub> and the C<sub>11</sub>–O<sub>10</sub> bond lengths are 1.347(4) and 1.364(4) Å, respectively.

The difference on reactivity of the  $[\text{OEPFe}^{\text{II}}\text{Cl}]$  species and that of  $[\text{OEPFe}^{\text{II}}\text{PF}_6]$  toward O<sub>2</sub> is remarkable. Whereas species containing strongly coordinating ligands, such as Cl, reacts rapidly with O<sub>2</sub> via a ring-centered reaction that results ultimately in a ring-opened oxidized product (an iron biliverdin-type complex),<sup>32</sup>  $[\text{OEPFe}^{\text{II}}\text{PF}_6]$ , which contains a weakly coordinating anion, reacts with dioxygen most

likely via a metal-centered reaction to give the  $\mu$ -oxo species  $[(\text{OEPFe})_2\text{O}](\text{PF}_6)_2$ . These results imply, therefore, that the site of oxygenation (ring vs metal) may be controlled by the nature of the axial ligand. That axial ligands are able to play significant roles in governing the oxidation chemistry of metalloporphyrins is well established.<sup>33</sup>

It is important to note that these results may have also some biological implications by shedding some light on verdoheme degradation to biliverdin. They suggest that the presence of strongly coordinating axial ligands during the oxidation of the verdoheme by the heme oxygenase system is likely essential to shift the oxygenation site from the metal center to the oxoporphyrin ring. Indeed, the high-spin ferrous center in verdoheme-heme oxygenase complexes are suggested to have a proximal histidine moiety and, possibly, a hydroxide ion as axial ligands.<sup>34, 35</sup>

**Acknowledgment.** We thank University of Sistan and Baluchestan for financial support. We thank Prof. B. R. James for his assistance. J.S.R. thanks the Natural Sciences and Engineering Research Council of Canada (NSERC) for support.

**Supporting Information Available:** Crystallographic data in CIF format. This material is available free of charge via the Internet at <http://pubs.acs.org>.

IC050211A

- (29) Strauss, S. H.; Pawlik, M. J.; Skowrya, J.; Kennedy, J. R.; Anderson, O. P.; Spertalian, K.; Dye, J. L. *Inorg. Chem.* **1987**, *26*, 724–730.  
 (30) Scheidt, W. R.; Summerville, D. A.; Cohen, I. A. *J. Am. Chem. Soc.* **1976**, *98*, 6623–6628.  
 (31) Scheidt, W. R.; Cheng, B.; Safo, M. K.; Cukiernik, F.; Marchon, J.-C.; Debrunner, P. G. *J. Am. Chem. Soc.* **1992**, *114*, 4420–4421.

- (32) Nguyen, K. T.; Rath, S. P.; Latos-Grażyński, L.; Olmstead, M. M.; Balch, A. L. *J. Am. Chem. Soc.* **2004**, *126*, 6210–6211.  
 (33) Brown, G. M.; Hopf, F. R.; Ferguson, J. A.; Meyer, T. J.; Whitten, D. G. *J. Am. Chem. Soc.* **1973**, *95*, 5939–5942.  
 (34) Yoshida, T.; Migita, C. T. *J. Inorg. Biochem.* **2000**, *82*, 33–41.  
 (35) Lad, L.; de Montellano, P. R. O.; Poulos, T. L. *J. Inorg. Biochem.* **2004**, *98*, 1686–1695.